SAND REPORT
SAND2002-4215
Unlimited Release
Printed December 2002

Use of Intense Ion Beams for Surface Modification and Creation of New Materials

Timothy J. Renk, Paula P. Provencio, Paul G. Clem, Somuri V. Prasad, and Michael O. Thompson

Prepared by
Sandia National Laboratories
Albuquerque, New Mexico 87185 and Livermore, California 94550

Sandia is a multiprogram laboratory operated by Sandia Corporation, a Lockheed Martin Company, for the United States Department of Energy under Contract DE-AC04-94AL85000.

Sandia National Laboratories

Issued by Sandia National Laboratories, operated for the United States Department of Energy by Sandia Corporation.

Available to DOE and DOE contractors from
U.S. Department of Energy
Office of Scientific and Technical Information
P.O. Box 62
Oak Ridge, TN 37831

Telephone: (865)576-8401
Facsimile: (865)576-5728
E-Mail: reports@adonis.osti.gov
Online ordering: http://www.doe.gov/bridge

Available to the public from
U.S. Department of Commerce
National Technical Information Service
5285 Port Royal Rd
Springfield, VA 22161

Telephone: (800)553-6847
Facsimile: (703)605-6900
E-Mail: orders@ntis.fedworld.gov
Online order: http://www.ntis.gov/ordering.htm

SAND2002-4215
Unlimited Release
Printed December 2002

Use of Intense Ion Beams for Surface Modification and Creation of New Materials

Timothy J. Renk
Beam Applications and Initiatives Department

Paula P. Provencio
Materials Aging & Reliability: Interfaces Department

Paul G. Clem and Somuri V. Prasad
Microsystems Materials, Tribology and Technology Department

Sandia National Laboratories
P. O. Box 5800
Albuquerque, NM 87185-1182

Michael O. Thompson
Department of Materials Science
Cornell University, Ithaca, NY 14853

Abstract

We have conducted surface treatment and alloying experiments with Al, Fe, and Ti-based metals on the RHEPP-1 accelerator (0.8 MV, 20 W, 80 ns FHWM, up to 1 Hz repetition rate) at Sandia National Laboratories. Ions are generated by the MAP gas-breakdown active anode, which can yield a number of different beam species including H, N, and C, depending upon the injected gas. Beams of intense pulsed high-power ion beams have been used to produce surface modification by changes in microstructure caused by rapid heating and cooling of the surface. Increase of beam power leads to ablation of a target surface, and redeposition of ablated material onto a separate substrate. Experiments are described in which ion beams are used in an attempt to increase high-voltage breakdown of a treated surface. Surface alloying of coated Pt and Hf layers is also described. This mixing of a previously deposited thin-film layer into a Ti-alloy substrate leads to significantly enhanced surface wear durability, compared to either untreated Ti-alloy alone, or the Ti alloy alone treated with the ion beam. Thin-film layers have been produced from a number of target materials. Films of fine-grain Pt and Er are described, and are compared to conventionally formed films. First attempts to form high-dielectric constant BaTiO3 are described.

Table of Contents

Use of Intense Ion Beams for Surface Modification and Creation of New Materials

I. Introduction

This is a report of results from a two-year LDRD project to investigate the use of intense pulsed ion beams for both surface modification, and creation of new thin-film materials. Such a beam incident on a surface will result in a rapid heating of the near-surface layer, as ions penetrate and deposit energy in a timescale that is short compared to thermal diffusion. Heat conduction into the substrate then leads to resolidification at quench rates that can exceed 10^9 K/sec. This rapid cooling can lead to the formation of non-equilibrium surface microstructures and metastable alloys not accessible by conventional alloying methods. Additional alloying elements can be added to the surface by the application of a separate thin-film layer to the substrate prior to beam treatment. During the power pulse, this film diffuses or convects into the substrate. The coating can be chosen to produce substantial improvements in surface properties beyond that possible by either conventional alloying or by intense beam treatment without the coating layer. This process will be referred to as *surface alloying*. For high enough beam power, the surface will be driven into ablation, and material can be collected on a substrate to form thin-film layers.

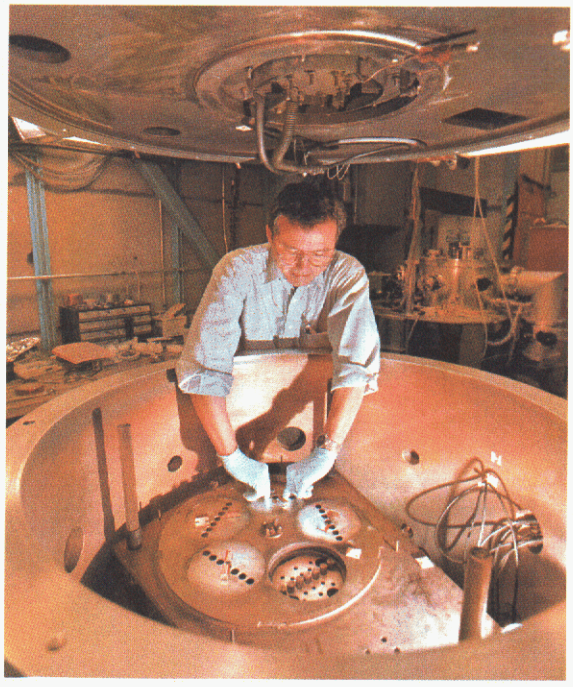

Figure I. Photograph of RHEPP-1 treatment vacuum tank. For thin-film deposition, the table shown is removed and ablation target substituted in its place.

Experiments in both surface modification and ablation/redeposition were conducted on the RHEPP-1 facility at Sandia National Laboratories. Fig. 1 shows a photograph of the treatment area. The top surface is the cathode, through which the beam propagates downward to the treatment table. Several sample trays are shown, each with a set of seven through-holes to Faraday cups which monitor the delivered ion beam dose. Typical deposited energies for surface modification are 2-5 J/cm^2. For the voltages and currents considered here (up to 700 kV and up to 200 A/cm^2 on RHEPP-1 over the 200 ns power pulse at the sample location), typical melt distances are ~ 2cm in metals such as Ti and Fe alloys. Previous surface modification and alloying experiments have been undertaken on RHEPP-1 [1,2]. Increasing the dose to 5-7 J/cm^2 results in ablation and redeposition of materials onto a separate substrate to form a thin-film layer. In this case, the table shown in

the figure is replaced by an ablation target. Such thin-film experiments have also been described elswhere[3]. We report here on the analysis of new and novel microstructures formed in such layers.

The sections below include a discussion of the experimental setup, description of the beam, and a description of the results to date of several investigation areas.

II. Experimental Setup

Figure 2 shows the treatment geometry. An annular beam of average radius 10 cm is generated from a magnetically insulated ion diode, and propagates to a target table located between 25 and 65 cm away. Insulation coils located on the cathode side suppress electron leakage current. The ion source, referred to as MAP (Magnetically confined Anode Plasma),

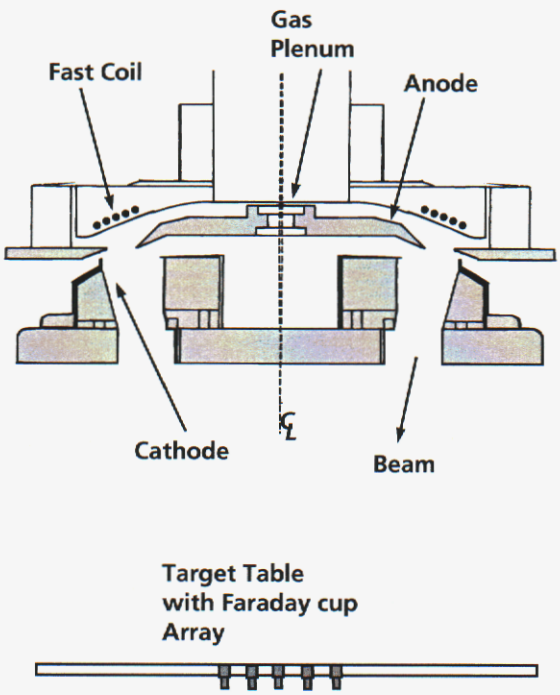

Figure 2 Diode Geometry including MAP ion source and treatment area.

consists of an axially located plenum valve and inner and outer flux excluders. Prior to the power pulse, the valve is energized, and gas expands radially towards the annular space between the flux excluders. A fast coil is pulsed which ionizes the gas, and the interaction of the fast coil magnetic field with the slower insulation field pushes the resulting plasma into position for acceleration when the power pulse arrives. A set of magnetically insulated Faraday cups (outfitted with permanent magnets) is mounted on the target table. The cups measure the total beam fluence as a function of position, and in addition are able to resolve different beam constituents through time-of-flight (TOF) analysis. For thin-film deposition, the table and cups are removed, and the ion beam dose estimated from prior experiments.

Beams were formed from different gases for the experiments described below. The motivation for beam use, and description of the beams used in each case is discussed below.

III. Use of ion beam surface modification to increase the high-voltage (HV) breakdown stand-off of Tri-Clad alloy and stainless steel 316LSCQ

The surface of manufactured and conventionally smoothed metals such as stainless steel typically will stand off a voltage of about 300-400 kV/cm before breakdown. The breakdown may be caused by any number of factors – surface topology, oxide layer formation, contamination such as fingerprints, dust, etc, and inclusions either of second-phase metals or dielectric material, either present from the manufacturing process or added as a result of mechanical polishing. We have studied the use of an argon ion beam to increase this breakdown value, in two application areas. Within the neutron tube (NT) program, there is a need to

increase the breakdown strength of Tri-Clad alloy used in NTs, to help extend their useful lifetime. Also, at present there is an ongoing investigation of the surface treatment of SS304 and 316LSCQ (low sulphur) using a combination of electron beam surface treatment (30 keV) and ion implantation. This investigation is being conducted at the High Current Electronics Institute in Tomsk, Russia. We have studied the use of ion beam treatment of SS316LSCQ in comparison with the electron beam/implantation process.

In the case of the NT Tri-Clad alloy, in initial experiments using a mixed carbon/argon ion beam, an electrode treated with a single ion pulse had shown promising increase in breakdown strength to 400 kV/cm. This beam was chosen because the heavier species produce a smoother treated surface than that produced by a proton beam. However, the sample treated with multiple pulses (38 shots) could not be tested similarly, because it evolved enough gas when subjected to pumpdown to raise the vacuum pressure from 10^{-5} to 10^{-8} Torr. This in itself is an interesting result, because it implies that the treatment beam can become incorporated into the treatment material in enough concentration to be detectable. Additional electrodes were treated with a predominantly carbon beam (no argon), to see if entrained Ar could have been the cause of the gas evolution. These electrodes have not yet been tested for breakdown strength. The reason is that the high-voltage fixturing used by the NT program to test for stand-off developed internal breakdowns that limited performance. In addition, performance problems with both the source and target thin films used in NTs became a higher-priority research issue, and so HV testing within the program was suspended. (See the discussion below about thin-film characterization.)

In the case of the SS316LSCQ, a sample of this alloy was treated with 25 pulses of the mixed carbon/argon beam. The high-voltage standoff failed to improve. The reason appears to be the presence of Cu particles, entrained within the treated surface, that have been carried by the treatment beam. These particles appear to be the initiation site of voltage breakdowns. The source of the Cu is wear within the diode due to improper source operation, and is being investigated separately. Meanwhile, another approach is being considered, that of adding a coating to the steel surface, and using the surface alloying technique to mix the added coating into the substrate. This is based upon the favorable smoothening/cratering reduction seen with the Hf/Ti surface alloying experiments described below. A 1 micron Cr coating has been applied to a SS316LSCQsample, and treatment is planned in the near future.

IV. Surface alloying of Pt and Hf into Ti alloy to improve surface wear durability

This is a follow-on to work previously done [1], in which a 1 micron layer of mixed Pt-Ti composition was applied to the surface of Ti-6-4 (Ti with 6% Al, 4% V), a common Ti alloy. In the previous work, wear durability of the treated sample was tested by a linear reciprocating tribometer using ball-on-flat geometry with a 440C steel counterface. The mixed Pt-Ti layer was found to withstand between 200 and 2000 cycles , compared to 20 for the untreated Ti-6-4, or the coated but untreated layer, before the friction coefficient increased significantly. Subsequent cross-sectional transmission electron microscopy (XTEM) showed the formation of a 1 micron-thick crystalline layer of metastable Pt, in solid solution (4-5 at% Pt) in an a-Ti lattice. This novel microstructure appears to be the source of the increased wear durability.

Samples of 1 micron-thick co-sputtered layers of mixed Pt and Ti were prepared,

on a Ti-6-4 substrate. The concentration of Pt was 10 at% in one case, and 20 at% in the other. Similar layers were prepared with Hf instead of Pt. Hf was chosen for investigation for two reasons: 1) Whereas Pt is almost insoluble in the low-temperature α-Ti crystal structure, Hf is soluble in both the α- and β-Ti forms. This natural alloying propensity may lead to a different microstructure in the treated layer; and 2) the Hf atom is larger than Ti, compared to the smaller size of the Pt atom. This could lead to different lattice strain behaviors.

The co-sputtered samples were treated with 35 pulses of the MAP nitrogen beam (beam composition almost evenly split between N+2 and N+1), in doses ranging from 1 to 4.5 J/cm^2. This type of beam was used in the original surface alloying experiments. Afterwards, selected portions were subjected to 1000 cycles of a linear reciprocating tribometer using a Si_3N_4 ball counterface with 10 gms force. The tribometer was operated in a dry nitrogen atmosphere. Tested areas included differing amounts of dose, as well as the coated but untreated surface.

Analysis is still underway on the wear tracks, but the treated coated surface, whether Pt or Hf, and with either the 10 or 20 at% concentration, showed consistently lower friction coefficients than the coated but untreated layer. Only the Hf 20 at% sample has been studied in detail with scanning electron microscopy (SEM). Figs. 3 show the behavior of the friction coefficient for the following surface conditions: 1) coated but untreated, and 2) doses of <1 J/cm^2, 1, 2.25, 2.8, and 3 J/cm^2. SEM images of four of the wear tracks are shown in Figs. 5 (page 10). The untreated wear track exhibits many debris particles, indicating rapid wear-through of the soft coating, as evidenced by a high friction coefficient (Fig. 3a). The wear track at the lowest dose shows many wear particles, of light color which appear to be Hf-rich. This indicates that

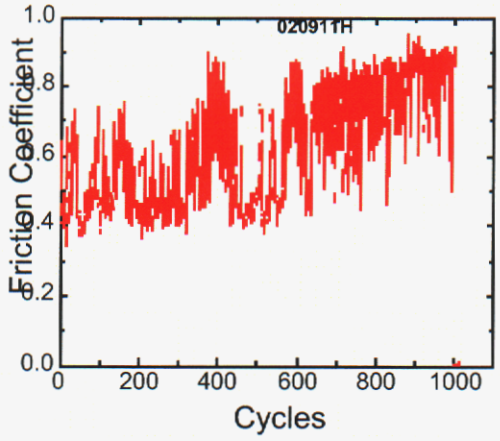

Figure 3a. Friction coefficient, coated but untreated Hf/Ti layer.

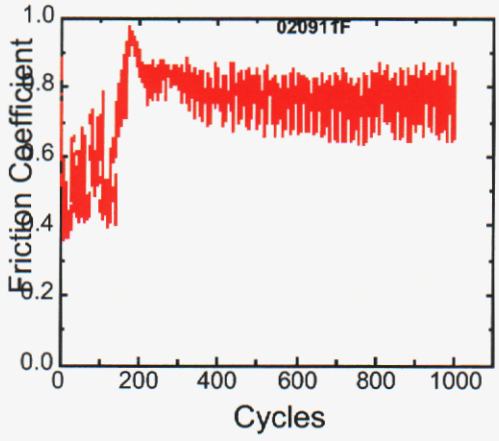

Figure 3b. Friction coefficient, treated with < 1 J/cm^2.

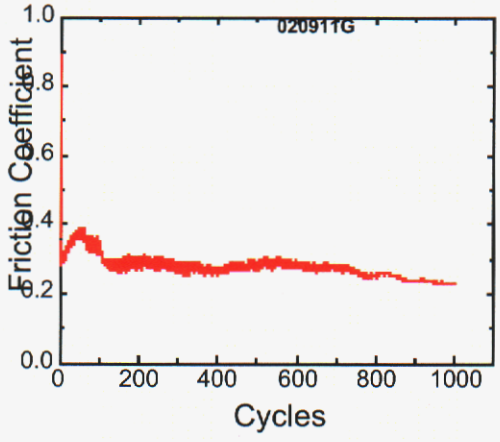

Figure 3c. Friction coefficient, treated with 1 J/cm^2.

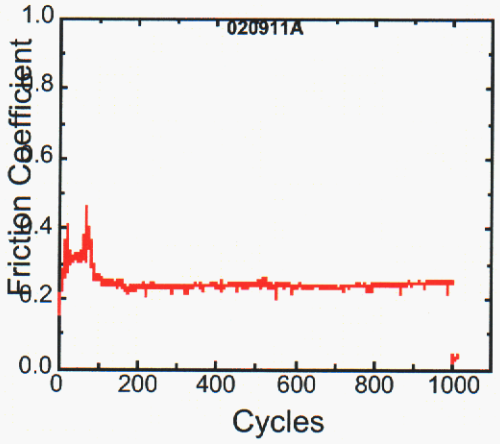

Figure 3d. Friction coefficient, treated with 2.25 J/cm^2.

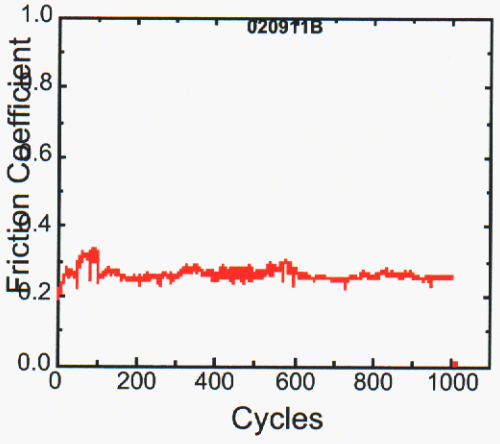

Figure 3e. Friction coefficient, treated with 2.8 J/cm^2.

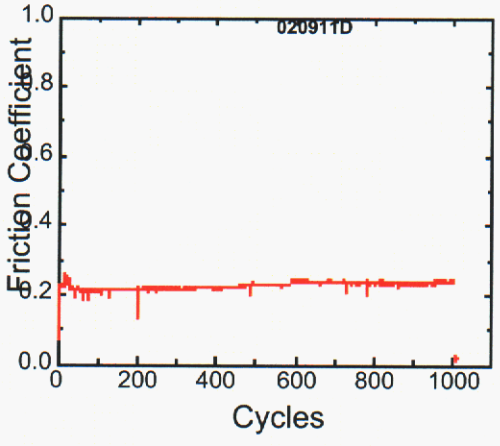

Figure 3f. Friction coefficient, treated with 3 J/cm^2.

the treatment dose is insufficient to mix the layer adequately. In addition, the surface morphology of the Hf layer at the lower treatment doses shows large 'mudcrack' structures. These probably do not interfere with the tribometer testing, and fade and disappear as the dose increases across the test specimen. These 'cracks', of unknown depth at present, are probably due to the initial difficulty in melting and mixing the Hf into the Ti material, since the melting melting point of Hf is significantly higher than the Ti (2500K compared to 1943K for Ti). The melting point of Pt (2045K) is much closer to that for Ti, and no 'cracks' were observed in the Pt/Ti samples.

At the higher treatment doses, the number and size of the light-color wear particles diminishes, and at the highest dose (3 J/cm^2), the track wear appears to be very slight, and with black residue instead of light-color particles. (SEM images are black-white false-color images, so that the color has no intrinsic meaning.) Analysis of the dark-color debris is in progress, but the indication is that the material is Si_3N_4 which has been worn off the counterface. If so, this would be a significant result, because it would indicate that the mixing of the Hf into the Ti-6-4 substrate has improved is surface durability to be conparable to or greater than Si_3N_4, which is well known as a hard surface.

A wear test was also conducted on an area of uncoated Ti-6-4 that was subjected to beam treatment. The behavior of the friction coefficient is shown in Fig. 4 on the next page. The dose at the track position was between 1 and 1.5 J/cm^2. As can be seen, the friction coefficient is high, compared even to the track on the coated/treated surface corresponding to 1 J/cm^2.

Another potentially very significant finding about the surface morphology of these samples is the presence and density of

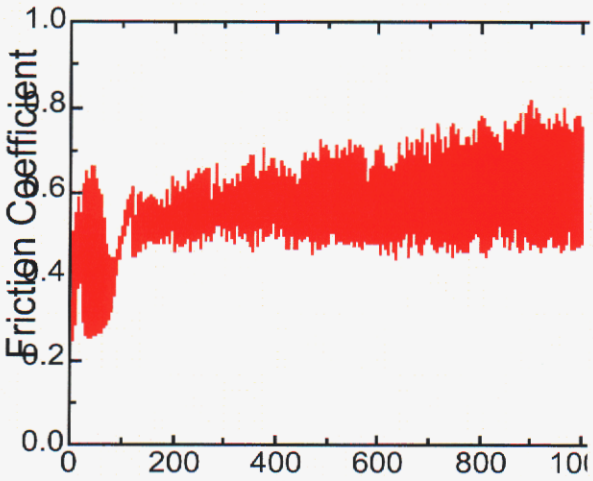

Figure4. Friction coefficient, uncoated Ti-6-4 treated with 1 - 1.5 J/cm^2.

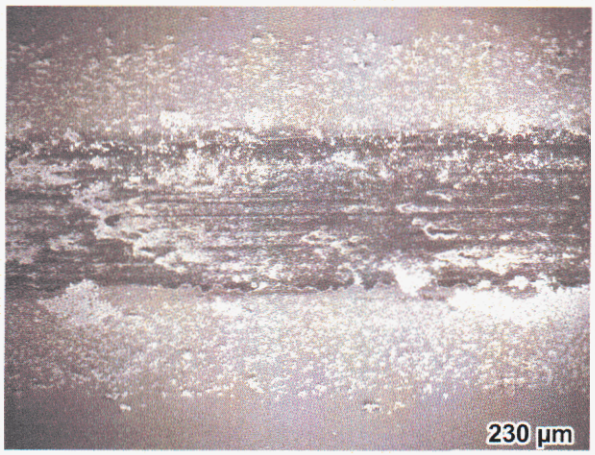

Figure 5a. Wear track, coated Hf/Ti but untreated.

surface craters. These are craters of symmetric shape, unlike those produced by material carried and deposited on the sample by the beam. The symmetric shape points to a materials response from the treated surface. Normally the cause of such craters can be liberated entrained gas in the substrate, vaporization of low-temperature alloying elements, etc. But this does not appear to be the case here. The observations are: 1) the Pt/Ti treated surface exhibits a 'speckly' appearance at higher dose

Figure 5d (right). Wear track, coated Hf/Ti treated with 3 J/cm^2.

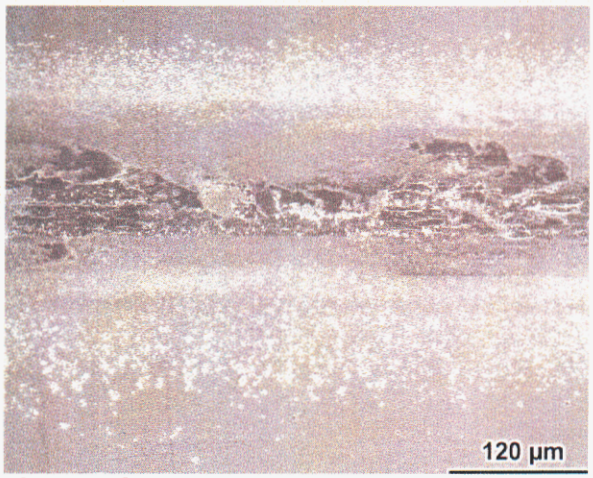

Figure 5b. Wear track, coated Hf/Ti treated with 1 J/cm^2.

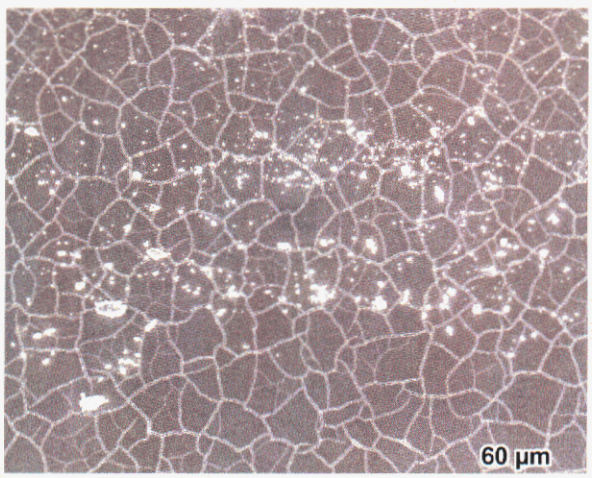

Figure 5c. Wear track, coated Hf/Ti treated with 2.25 J/cm^2.

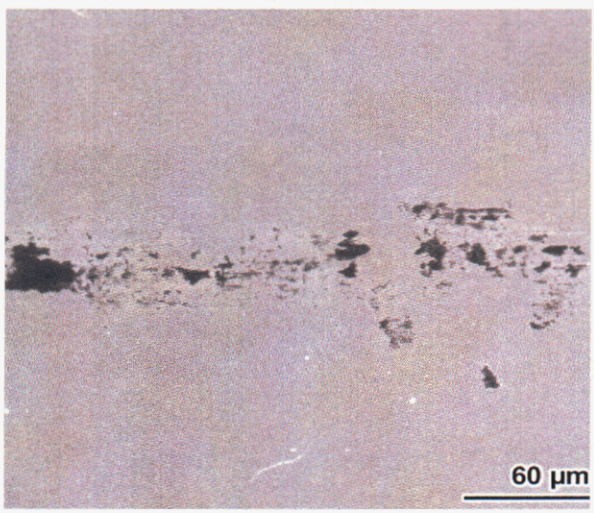

(above ~ 1.5J/cm^2). Observation with a low-power optical microscope (10X or 20X) shows these speckles to be craters. 2) These craters are absent from the Hf/Ti samples. In addition, 3) in portions of the Hf/Ti samples (in the low dose treated areas), the Hf coating was delaminated from the sample. This delamination is confirmed by profilometer scans across the interface, which show a 1 micron height difference. It is unknown at what point in the 35 shot series the coating delaminated, and so an unknown amount of the Hf/Ti sputtered layer may be diffused into the substrate. It is observed that the crater density is higher in the delaminated region, even compared to a region just across the interface, in which the coating still remains.

The origin of this cratering difference is unknown. The substrate in all cases is identical, and the only added material is from the co-sputtering, either Pt or Hf, in either 10 or 20 at% concentrations, in a 1 micron-thick layer. (The atomic % translates to a much higher weight % of either Pt or Hf, since both are much higher density metals than Ti.) These observations suggest that extended study of cratering is needed, which is outside the scope of this paper.

V. Production of nanocrystalline thin films by pulsed ion beam deposition (PIBD)

Thin films are produced conventionally by two main techniques. One approach is unbalanced magnetron sputtering. A low energy (few keV) ion beam inpinges on the surface, sputtering off the target material to form a thin film on a collection substrate. Electron beam evaporation is the second technique. In both cases, the deposition ions produced have an energy on the order of a fraction of an eV. A third technique, pulsed laser deposition (PLD), produces higher energy deposition ions (few eVto tens of eV). The microstructure produced by PLD can differ from that produced by the two conventional techniques. For example, the grain size in the thin film may be smaller.

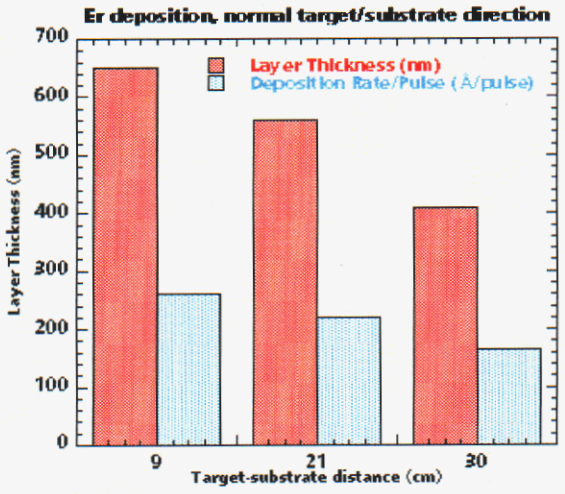

Figure 6a. Layer thickness (25 pulses) and per-pulse deposition rate for ablation of an Er target, as a function of target-substrate distance

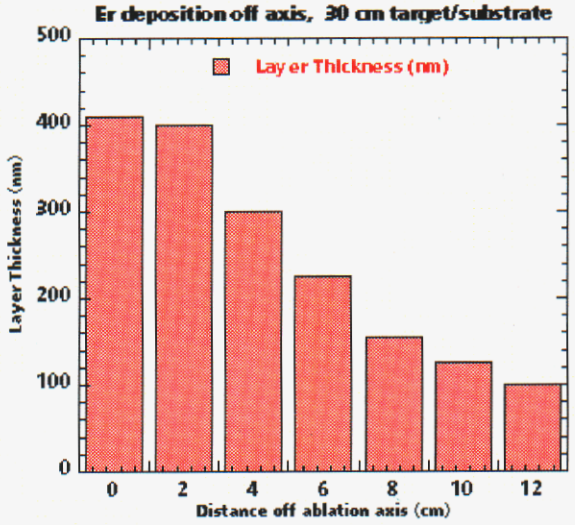

Figure 6b. Layer thickness (25 pulses), Er target, as a function of distance away from ablation axis. Here target-substrate distance is 30 cm.

Pulsed ion beam deposition can produce a high energy plasma plume similar to

that produced by PLD. But the amount of thin film area produced by PLD (throughput) is limited, because in order to generate high ablation power with lasers, the beam spot size must be small (~ mm area). The resulting deposition rate is usually on the order of 1 Å/pulse. Even at a pulse rate of 5 Hz, this deposition rate is rather low. The area of an ion beam that can ablate a target can be much larger (tens of cm^2). On RHEPP-1, we have measured deposition rates as high as 0.5 microns/pulse. In addition, the ablation plume created by the PIBD pulse has a large angular spread, i.e. at an angle of 30 degrees off the ablation axis, the deposition rate may only decrease by 50%. This allows a large solid angle of deposition substrates, and hence PIBD can scale to a much higher throughput rate than PLD, by several orders of magnitude.

An example of the deposition behavior on RHEPP-1 can be seen in Figs. 6. Fig. 6a shows the deposited layer thickness for 25 shots, and the deposition rate per shot, for ablation of an Er target. Distances shown are from the ablation target to the deppositional substrate. Note the high deposition rate, even for a target-substrate distance of 30 cm. The Er in this case is a standard 2 inch sputter target. Even higher deposition rates can be expected with a larger ablation target.

Fig. 6b shows the deposition behavior for distances away from the ablation axis, i.e. a line normal to the ablation target surface. In this case, the target-substrate distance is 30 cm. The inferred ablation plume angular distance is on the order of 30 degrees. This again shows the large amount of deposited material made possible by PIBD.

The high deposition rate also can lead to a fundamentally different film microstructure from the other techniques. This is because almost all conventionally deposited films increase in thickness by 'island growth'. That is, the deposition is at first not continuous over the deposition surface, because of the low deposition rate. Islands of material form at first, and then these islands coelesce as the film gets thicker. This lead almost inevitably to columnar grain structure, i.e. vertically-tending grains, where the grain boundaries are oriented away from the substrate surface, and towards the film surface.

The films we have produced by PIBD, however, do not tend to be columnar, with large grains, but instead have a more nano-crystalline grain structure. It appears that that the high deposition rate is the main reason.

Va. Pt films produced by PIBD, compared with magnetron sputtered films

We have produced thin films of Pt, on Si(100) single-crystal (wafer) substrate. The PIBD films were produced by using a 2 inch beam target of pure Pt. The diode-target distance was 40 cm, and the distance from target to substrate was 28 cm. A mixed proton-carbon beam (30% H, the rest in C+2 and C+1 charge states) was used to produce the films. This beam was chosen because the delivered dose is the highest of the beams available, which should maximize ablation. A similar film was produced by unbalanced magnetron sputtering. Samples were prepared both at room temperature (RT), and at 250C. The sputtered samples were furnished by Dr. Midori Kawamura (Kitami Institute of technology, Kitami, Japan). We had initially attempted thin film formation at 350C, but XTEM analysis showed the presence of Pt silicides. This indicates that interdiffusion was taking place at the coating boundary. In order to avoid this, we lowered the heating temperature to 250C. In the case of the PIBD film, 75 shots were needed to make a 1 micron-thick Pt film, or about 13 nm/pulse deposition rate.

Samples were sectioned and examined by XTEM. Figs. 7a and 7b show the grain structures in the PIBD-produced films and the

Figure 7a. XTEM cross-sectional view of PIBD-deposited Pt. Note the fine grain structure of the layer.

Figure 7b. Pt layer deposited by unbalanced magnetron sputtering. Note the large and columnar grain structure.

sputtered films, respectively. Note that thePIBD film is nanocrystalline, with typical grain size ~ 10 nm. Furthermore, the crystal orientation is random, and in particular, there are no direct paths to the surface along grain boundaries. The sputtered film exhibits large-scale grains, of order 50 - 100 nm, and oriented vertically. The PIBD film produced at room temperature exhibits the largest dislocation density. In the case of the heated films (250C), the grain size becomes larger in both cases. The sputtered film shows more dislocations at 250C than the RT sample, whereas the elevated temperature PIBD sample showed reduced dislocation density. The reason for the opposite scaling of dislocations is unknown.

Vb. Er films produced by PIBD, compared with electron beam evaporated films

Similar deposition experiments were conducted with Er film formation. In place of the Pt, a same-size disk of Er was substituted. The PIBD geometry remained the same. In place of the sputtered Pt film, we examined Er films made by the standard electron-beam evaporation process used to make Er thin films in the neutron tube program. The substrate in this case was polycrystalline Mo. Similar to the Pt case, the PIBD-produced Er film is nanocrystalline, with typical grain size 10 nm. The evaporated layer, while exhibiting much narrower grains than in the case of the Pt above, shows a tall vertical-tending microstructure similar to that seen with the sputtered Pt layer.

The fine grain structure of the PIBD-produced Er is promising, because the layer may prove superior to the standard film in its ability to retain He. This is a significant problem with recent Er films produced within the NT program. When loaded with tritium, the films initially perform well, but when the tritium decays to He, the latter is insoluble in the Er film, and diffuses out of the layer, mainly along grain boundaries. The vertical nature of the grain structure apparently facilitates this process. Several possible solutions to this problem have been suggested: 1) make the grain horizontal-tending, or possibly smaller,

2) increase dislocations, and 3) dope the film with other elements which may reduce He diffusivity. The PIBD-produced Er layer thus looks promising as an alternative to the standard Er layer.

Regarding film doping, there is evidence from Russian work sponsored by SNL [Surenyants et al, ISTC 323-96 (1999)] that addition of Al to the Er film may retard the release of He. In the PIBD process, the film can be potentially easily doped by adding a small amount of the doping material to the ablation target. Since the ablation plumes from the Er and Al may have different velocities, carfeful post-analysis will have to establish whether simple composite target use is succesful, or whether the Er and Al must be mixed more thoroughly in the ablation target.

An Er layer doped with Al has been produced and has been studiedby XTEM. The film has similar microstructure to teh Er-only film, as would be expected. Further analysis will be required to determine the effect of the Al addition to the film.

In addition to Er target films, a single sample of Sc source film has been produced by PIBD, and has been studied by XTEM. The substrate in this case is a ceramic doped with Mo. The grain size here is even finer than with the Er.

Vc. Production of BaTiO3 films by PIBD of high dielectric constant for energy storage applications

Four trends driving capacitor fabrication are higher capacitance densities, thinner dielectric layers, lower operating voltages, and lower cost electrode materials. Materials based on $BaTiO_3$ (BT) display high dielectric constants, low leakage currents, and low dielectric losses, properties desired for many applications, including decoupling capacitors for integrated circuits, and DC buss capacitors for hybrid and fuel cell electric vehicles. For both of these applications, ability to produce low cost, high capacitance, low loss capacitors with good temperature stability (-55 C to 125 C) is of interest. One class of $BaTiO_3$ compositions, denoted X7R, display a dielectric constant that varies less than 10% from –55 C to 125 C. In the present research, a powder bed of this composition, with a bulk dielectric constant of 2650, was pressed to form a four inch round target, and annealed at 900 C to partially densify the target. This composition was then deposited by PIBD onto silicon wafers coated with a platinum bottom electrode (1700A Pt/300A Ti/3000nm SiO_2/Si wafer). Following deposition of the $BaTiO_3$ dielectric on the platinized silicon substrate, top platinum electrodes were RF sputtered through shadow masks to define 500mm top electrodes, and define parallel plate capacitors. These capacitors were then analyzed by a Hewlett-Packard 4284A Precision LCR meter to determine both the capacitance (C) and the dissipation factor, the ratio of charge conducted to charge stored. The dielectric constant can then be determined, given the capacitor area and thickness.

Initial capacitors tested were completely short circuited; this was likely the result of porosity within the deposited film, and platinum filling this porosity during deposition of the top electrode. In the second round of $BaTiO_3$ capacitor deposition, the yield of capacitors was low (~ 10% were not shorted), with measurable values. Films of 670nm-thick $BaTiO_3$ deposited at room temperature displayed a 1 kHz permittivity e' = 41.5 and dissipation factor of 15%. After annealing the capacitors at 700 C for 30 minutes, the film appeared to densify, and yielded a 1 kHz permittivity e' = 308 and dissipation factor = 5.2%. In a second set of films, deposited at 200 C, the as-processed 822nm-thick films displayed a 1 kHz permittivity e' = 37 and dissipation factor = 20%. After a 700C, 30 minute crystallization anneal, the

films displayed a 1 kHz permittivity e' = 240 and dissipation factor = 3.8%. If the yield of these films can be improved, and high deposition rates maintained, this could be a promising method of high rate dielectric deposition for integrated thin film capacitors in the 100 nF – 1 mF range.

VII. Summary

We have conducted surface treatment and alloying experiments with Al, Fe, and Ti-based metals on the RHEPP-1 accelerator (0.8 MV, 20 W, 80 ns FHWM, up to 1 Hz repetition rate) at Sandia National Laboratories. Ions are generated by the MAP gas-breakdown active anode, which can yield a number of different beam species including H, N, and C, depending upon the injected gas. Beams of intense pulsed high-power ion beams have been used to produce surface modification by changes in microstructure caused by rapid heating and cooling of the surface. Increase of beam power leads to ablation of a target surface, and redeposition of ablated material onto a separate substrate. Treatment with the RHEPP ion beam to raise high-voltage breakdown has been partially successful, and seems limited by the presence of Cu in the beam. Surface alloying of coated Pt and Hf layers has led to mixing of a previously deposited thin-film layer into a Ti-alloy substrate, resulting in significantly enhanced surface wear durability. Thin-film layers have been produced from a number of target materials. Films of fine-grain Pt and Er have been produced, as compared to conventionally formed films. First attempts to form high-dielectric constant BaTiO3 have been achieved.

VIII. Acknowledgement

Gerard Torres and Gregory Mann provided able technical assistance for theRHEPP-1 experiments.

This work was supported by the United States Department of Energy under Contract DE-AC04-94AL85000. Sandia is a multi-program laboratory operated by Sandia Corporation, a Lockheed Martin Company, for the United States Department of Energy.

VIIII. References

1. T. J. Renk, R. G. Buchheit, N.R. Sorensen, D. Cowell Senft, M. O. Thompson, and K. S. Grabowski, Physics of Plasmas **5**, 2144 (1998).

2. A. D. Pogrebnyak, Phys. Stat. Sol. (a) **117**, 17 (1990).

3. K. Yatsui, X. D. Kang, T. Sonegawa, T. Matsuoka, K. Masugata, Y. Shimotori, T. Satoh, S. Furuuchi, Y. Ohuchi. T. Takeshita, and H. Yamamoto, Phys. Plasma **1**, 1730 (1994).

DISTRIBUTION

Unclassified Unlimited Release

1	MS9018	Central Technical Files, 8945-1
2	MS0899	Technical Library, 96
1	MS0612	Review & Approval Desk, 9612 For DOE/OSTI

10 Prof. Michael O. Thompson
Department of Materials Science
Bard Hall
Cornell University
Ithaca, NY 14853

1 Dr. Walter M. Polansky
DOE/ER-32

Internal Distribution

1	MS0511	C. E. Meyers, 1010
10	MS1421	P. P. Provencio, 1122
1	MS1421	G. A. Samara, 1122
10	MS0889	S. V. Prasad, 1851
1	MS0889	R. J. Salzbrenner, 1851
20	MS1182	T. J. Renk, 15335
10	MS1182	B. N. Turman, 15335
1	MS1153	M. T. Buttram, 15330
1	MS1165	W. Guyton, 15300
1	MS1186	T. A. Mehlhorn, 1674
1	MS1188	C. L. Olson, 1600
1	MS1190	J. P. Quintenz, 1600